Preparation of Cationic Dinuclear Hydrido Complexes of Ruthenium, Rhodium, and Iridium with Bridging Thiolato Ligands and Their Reactions with Nitrosobenzene

Takafumi Iwasa, Hitoshi Shimada, Atsushi Takami, Hiroyuki Matsuzaka,† Youichi Ishii, and Masanobu Hidai*

Department of Chemistry and Biotechnology, Graduate School of Engineering, The University of Tokyo, Hongo, Bunkyo-ku, Tokyo 113-8656, Japan

Received November 2, 1998

A series of cationic dinuclear hydrido complexes with bridging thiolato ligands [Cp*MH(μ-SPr^i)$_2$MCp*][OTf] (**4**, M = Ru; **6a**, M = Rh; **7a**, M = Ir; Cp* = η^5-C$_5$Me$_5$, OTf = OSO$_2$CF$_3$) were synthesized by treatment of the corresponding chloro complexes [Cp*RuCl(μ-SPr^i)$_2$Ru(OH$_2$)Cp*][OTf] (**1**) or [Cp*M(μ-Cl)(μ-SPr^i)$_2$MCp*][OTf] (**2**, M = Rh; **3**, M = Ir) with HSiEt$_3$. The dirhodium and diiridium complexes **6** and **7** have been shown to possess a bridging hydrido ligand by crystallographic analysis, while the diruthenium complex **4** is proposed to have a terminal hydrido ligand that undergoes facile migration between the two ruthenium centers in solution. Complexes **4**, **6a**, and **7a** reacted with nitrosobenzene to give the paramagnetic dinuclear nitrosobenzene complexes [Cp*M(μ-PhNO)(μ-SPr^i)$_2$MCp*]$^+$ (M = Ru, Rh, Ir) along with azoxybenzene. The molecular structures of the three nitrosobenzene complexes have been determined by X-ray diffraction study to reveal that in each case nitrosobenzene acts as a μ-η^1:η^1-*N*,*O* ligand. Judging from the molecular structures and the ESR spectra, the unpaired electron is considered to be located mainly on the nitrosobenzene ligand, at least in the diruthenium and dirhodium complexes. On the other hand, complex **2** reacted with nitrosobenzene to give the incomplete cubane-type trinuclear cluster [(Cp*Rh)$_3$(μ-Cl)$_2$(μ_3-S)(μ-SPr^i)]$^+$, whose molecular structure has also been determined crystallographically.

Introduction

The syntheses and reactivities of multinuclear complexes have been attracting intensified attention in recent years. Interests in multinuclear complexes stem from, at least in part, the view that activation of a substrate molecule at the multimetallic coordination site may lead to unique transformation of the substrate, which cannot be achieved at a monometallic coordination site.[1] We have centered our research activity on the chemistry of multinuclear complexes of groups 8−10 noble metals with bridging sulfur ligands[2−5] since this class of compounds is expected to provide robust multimetallic sites for unique chemical transformations.[2a,b,6] As a part of this ongoing investigation, we have synthesized a series of dinuclear complexes composed of Cp*Ru, Cp*Rh, or Cp*Ir (Cp* = η^5-C$_5$Me$_5$) units and bridging thiolato, hydrosulfido, disulfido, and/or polysulfido ligands and studied their chemical properties.[2a−h,3−5] As a consequence, these types of complexes, such as [Cp*RuCl(μ-SPr^i)$_2$Ru(OH$_2$)Cp*][OTf] (**1**, OTf = OSO$_2$CF$_3$),[3] have been shown to exhibit notable reactivities toward a wide variety of organic substrates at their dinuclear coordination sites.

Very recently, Na−Hg reduction of the dinuclear Ir(III)−Ir(III) complex [Cp*IrCl(μ-SPr^i)$_2$IrClCp*] has led to the formation of the dinuclear Ir(II)−Ir(II) complex [Cp*Ir(μ-SPr^i)$_2$IrCp*],[4,5] which is further converted into the cationic hydrido complex [Cp*Ir(μ-H)(μ-SPr^i)$_2$IrCp*][OCOCF$_3$] upon reaction with CF$_3$COOH.[4] Various reactivities observed at the cationic diruthenium core of complex **1** prompted us to synthesize the analogous cationic dinuclear hydrido complexes of ruthenium and rhodium. Now, we have found that a series of the hydrido complexes of the form [Cp*MH(μ-SPr^i)$_2$MCp*][OTf] (M = Ru, Rh, Ir) can readily be obtained by treatment of **1** or [Cp*M(μ-Cl)(μ-SPr^i)$_2$MCp*][OTf] (**2**, M = Rh; **3**, M = Ir) with HSiEt$_3$.

† Present address: Department of Chemistry, Tokyo Metropolitan University, Minami-osawa, Tokyo 192-0397, Japan.

(1) (a) In *Catalysis by Di- and Polynuclear Metal Cluster Complexes*; Adams, R. D., Cotton, F. A., Eds.; Wiley-VCH: New York, 1998. (b) Süss-Fink, G.; Meister, G. *Adv. Organomet. Chem.* **1993**, *35*, 41−134.

(2) (a) Hidai, M.; Mizobe, Y.; Matsuzaka, H. *J. Organomet. Chem.* **1994**, *473*, 1−14. (b) Hidai, M.; Mizobe, Y. In *Transition Metal Sulfur Chemistry: Biological and Industrial Significance*; Stiefel, E. I., Matsumoto, K., Eds.; ACS Symposium Series 653; American Chemical Society: Washington, DC, 1996; pp 310−323. For more recent reports, see: (c) Tang, Z.; Nomura, Y.; Ishii, Y.; Mizobe Y.; Hidai, M. *Inorg. Chim. Acta* **1998**, *267*, 73−79. (d) Kuwata, S.; Andou, M.; Hashizume, K.; Mizobe, Y.; Hidai, M. *Organometallics* **1998**, *17*, 3429−3436. (e) Kuwata, S.; Hidai, M. *Chem. Lett.* **1998**, 885−886. (f) Tang, Z.; Nomura, Y.; Kuwata, S.; Ishii, Y.; Mizobe Y.; Hidai, M. *Inorg. Chem.* **1998**, *37*, 4909−4920. (g) Masui, D.; Ishii, Y.; Hidai, M. *Chem. Lett.* **1998**, 717−718. (h) Qü, J.-P.; Masui, D.; Ishii, Y.; Hidai, M. *Chem. Lett.* **1998**, 1003−1004. (i) Mizobe, Y.; Hosomizu, M.; Hidai, M. *Inorg. Chim. Acta* **1998**, *273*, 238−243. (j) Ikada, T.; Kuwata, S.; Mizobe, Y.; Hidai, M. *Inorg. Chem.* **1998**, *37*, 5793−5797. (k) Takemoto, S.; Kuwata, S.; Nishibayashi, Y.; Hidai, M. *Inorg. Chem.* **1998**, *37*, 6428−6434. (l) Ikada, T.; Kuwata, S.; Mizobe, Y.; Hidai, M. *Inorg. Chem.* **1999**, *38*, 64−69.

(3) (a) Matsuzaka, H.; Takagi, Y.; Hidai, M. *Organometallics* **1994**, *13*, 13−15. (b) Matsuzaka, H.; Takagi, Y.; Ishii, Y.; Nishio, M.; Hidai, M. *Organometallics* **1995**, *14*, 2153−2155. (c) Shimada, H.; Qü, J.-P.; Matsuzaka, H.; Ishii, Y.; Hidai, M. *Chem. Lett.* **1995**, 671−672. (d) Nishibayashi, Y.; Yamanashi, M.; Takagi, Y.; Hidai, M. *Chem. Commun.* **1997**, 859−860. (e) Takagi, Y.; Matsuzaka, H.; Ishii, Y.; Hidai, M. *Organometallics* **1997**, *16*, 4445−4452.

(4) Nishio, M.; Matsuzaka, H.; Mizobe, Y.; Hidai, M. *Inorg. Chim. Acta* **1997**, *263*, 119−123.

(5) (a) Nishio, M.; Matsuzaka, H.; Mizobe, Y.; Hidai, M. *Angew. Chem., Int. Ed. Engl.* **1996**, *35*, 872−874. (b) Nishio, M.; Mizobe, Y.; Matsuzaka, H.; Hidai, M. *Inorg. Chim. Acta* **1997**, *265*, 59−63.

(6) Rakowski DuBois, M. *Chem. Rev.* **1989**, *89*, 1−9.

10.1021/ic981274e CCC: $18.00
Published on Web 05/20/1999

Coordination chemistry of C-nitroso compounds, most typically nitrosobenzene, has been investigated extensively over the past thirty years. Complexes of C-nitroso compounds show considerable structural diversity,[7] and they also provide coordination models for dioxygen complexes[8] and intermediates of catalytic reduction and reductive carbonylation of nitroarenes.[9] However, complexes in which nitrosobenzene acts as a bridging ligand have been relatively limited in number. We have observed that the cationic hydrido complexes obtained herein react with nitrosobenzene to form dinuclear μ-η^1:η^1-PhNO-*N*,*O* complexes of ruthenium, rhodium, and iridium. On the other hand, the reaction of complex **2** with nitrosobenzene gives rise to a novel cuboidal trirhodium cluster. This paper describes the synthesis of cationic dinuclear hydrido complexes of ruthenium, rhodium, and iridium with bridging thiolato ligands and their reactions with nitrosobenzene.

Experimental Section

General Considerations. All manipulations were performed using standard Schlenk tube techniques. Complex **1**[3a] and [Cp*IrCl(μ-SPr^i)$_2$IrClCp*][4] were prepared according to literature methods. The dirhodium complex [Cp*RhCl(μ-SPr^i)$_2$RhClCp*] was prepared from [Cp*RhCl$_2$]$_2$[10] and Pr^{i}SH by a similar procedure to that reported for the diiridium analogue.[4] Solvents were dried and distilled prior to use. Alumina for column chromatography was purchased from MERCK (Aluminum oxide 90). Other reagents were commercially obtained and used without further purification. IR spectra were recorded on a Shimadzu 8100M spectrometer. ^{1}H NMR spectra were obtained on a JEOL EX-270 or a JEOL JNM-LA 400 spectrometer. Amounts of the solvent molecules in the crystals were determined not only by elemental analyses but also by ^{1}H NMR spectroscopy. ESR spectra were acquired at room temperature on a JEOL JES-RE1X spectrometer. Quantitative GLC analyses of liquid products were performed on a Shimadzu GC-14A instrument equipped with a flame ionization detector, using a 25 m $\times$ 0.25 mm CBP10 fused silica capillary column, while GLC analyses of gaseous products were determined on a Shimadzu GC-8A instrument equipped with a thermal conductivity detector, using a Molecular Sieve 13X column. GC−MS analyses were carried out on a Shimadzu GCMS-QP5000 spectrometer. Elemental analyses were performed on a Perkin-Elmer 2400II CHN analyzer (for C, H, and N) or at the Elemental Analysis Laboratory, Department of Chemistry, Faculty of Science, The University of Tokyo (for Cl and S). Cyclic voltammetry measurements were carried out with Hokuto Denko instrumentation (HA-501 potentiostat and HB-105 function generator) by using a glassy carbon working electrode; potentials were measured in CH_2Cl_2/0.1 M [Bu$^n_4$N][BF_4] vs a SCE. Electroconductivities were recorded on a Toa CM-20A digital conductivity meter.

Preparation of [Cp*RuH(μ-SPr^i)$_2$RuCp*][OTf] (4). To a solution of **1** (99.9 mg, 0.121 mmol) in CH_2Cl_2 (5 mL) was added $HSiEt_3$ (0.19 mL, 1.2 mmol), and the mixture was stirred at room temperature for 20 h. During this period, the color of the solution changed from dark red-brown to dark brown. Addition of hexane to the concentrated solution gave **4** as dark brown microcrystals (81.6 mg, 0.106 mmol, 87%). IR (KBr disk, cm^{-1}): 1968, 1962 (CH_2Cl_2) [ν(Ru−H)].^{1}H NMR (CD_2Cl_2): δ −13.56 (s, 1H, Ru−*H*), 0.99 (d, 12H, J = 6.8 Hz, SCH*Me*$_2$), 1.75 (s, 30H, Cp*), 3.31 (sep, 2H, J = 6.8 Hz, SC*H*Me$_2$). Anal. Calcd for $C_{27}H_{45}F_3O_3Ru_2S_3$: C, 41.95; H, 5.87. Found: C, 41.90; H, 5.81.

Preparation of [Cp*RuH(μ-SPr^i)$_2$Ru(NCMe)Cp*][OTf] (5). Complex **4** (104.2 mg, 0.135 mmol) was dissolved in acetonitrile (3 mL) and stirred at room temperature for 1 h. The solvent was removed in vacuo, and the residue was dissolved in THF. Addition of hexane to the THF solution gave **5** as dark brown crystals (95.0 mg, 0.117 mmol, 87%). IR (KBr disk, cm^{-1}): 1943 [ν(Ru−H)].^{1}H NMR (CD_2Cl_2, −40 °C): δ −15.51 (s, 1H, Ru−*H*), 1.26, 1.29 (d, 6H each, J = 6.9 Hz, SCH*Me*$_2$), 1.58, 1.78 (s, 15H each, Cp*), 2.14 (sep, 2H, J = 6.9 Hz, SC*H*Me$_2$), 2.30 (s, 3H, *Me*CN). Anal. Calcd for $C_{29}H_{48}F_3NO_3Ru_2S_3$: C, 42.79; H, 5.94; N, 1.72. Found: C, 42.72; H, 5.94; N, 1.60.

Preparation of [Cp*Rh(μ-H)(μ-SPr^i)$_2$RhCp*][OTf] (6a) and [Cp*Rh(μ-H)(μ-SPr^i)$_2$RhCp*][BPh$_4$]·0.5(CH_2Cl_2) (6b·0.5(CH_2Cl_2)). To a suspension of [Cp*RhCl(μ-SPr^i)$_2$RhClCp*] (105.7 mg, 0.152 mmol) in THF (3 mL) was added a solution of AgOTf (39.1 mg, 0.152 mmol) in THF (6 mL), and the mixture was stirred at room temperature for 3 h. The white precipitate formed was filtered off, and the solvent was removed in vacuo. The resulting solid was then extracted with THF. Addition of ether to the concentrated extract gave complex **2** as a red crystalline solid (109.5 mg, 0.135 mmol, 89%). ^{1}H NMR (acetone-d_6): δ 1.38, 1.49 (d, 6H each, J = 6.9 Hz, SCH*Me*$_2$), 1.73 (s, 30H, Cp*), 3.13, 3.27 (br, 1H each, SC*H*Me$_2$). Anal. Calcd for $C_{27}H_{44}ClF_3O_3Rh_2S_3$: C, 39.98; H, 5.47. Found: C, 39.84; H, 5.67.

Complex **2** (104.4 mg, 0.129 mmol) and $HSiEt_3$ (0.20 mL, 1.3 mmol) were dissolved in THF (5 mL), and the mixture was stirred at room temperature for 20 h. During this period, the color of the solution changed from red to dark red-purple. Addition of hexane to the concentrated solution gave complex **6a** as dark brown microcrystals (93.8 mg, 0.121 mmol, 94%). ^{1}H NMR (CD_2Cl_2): δ −13.40 (t, 1H, J_{Rh-H} = 23.2 Hz, Rh−*H*), 1.06, 1.22 (d, 6H each, J = 6.8 Hz, SCH*Me*$_2$), 1.98 (s, 30H, Cp*), 2.07, 2.70 (sep, 1H each, J = 6.8 Hz, SC*H*Me$_2$). Anal. Calcd for $C_{27}H_{45}F_3O_3Rh_2S_3$: C, 41.76; H, 5.84. Found: C, 42.08; H, 5.60. The corresponding [BPh_4]$^-$ salt **6b**·0.5(CH_2Cl_2), which was used for crystallographic study, was obtained as dark red crystals by anion metathesis of **6a** with $NaBPh_4$ in THF and recrystallization from CH_2Cl_2/hexane.

Preparation of [Cp*Ir(μ-H)(μ-SPr^i)$_2$IrCp*][OTf] (7a) and [Cp*Ir(μ-H)(μ-SPr^i)$_2$IrCp*][BF_4] (7b). To a suspension of [Cp*IrCl(μ-SPr^i)$_2$IrClCp*] (101.0 mg, 0.115 mmol) in THF (3 mL) was added a solution of AgOTf (31.0 mg, 0.121 mmol) in THF (6 mL), and the mixture was stirred at room temperature for 24 h. White precipitate formed was removed by filtration, the solvent was removed in vacuo, and the resulting solid was extracted with THF. Addition of ether to the concentrated extract gave complex **3** as a yellow crystalline solid (99.4 mg, 0.100 mmol, 87%). ^{1}H NMR (acetone-d_6): δ 1.44 (br, 12H, SCH*Me*$_2$), 1.82 (s, 30H, Cp*), 3.2−3.4 (very br, 2H, SC*H*Me$_2$). Anal. Calcd for $C_{27}H_{44}ClF_3Ir_2O_3S_3$: C, 32.77; H, 4.48. Found: C, 32.94; H, 4.54.

Complex **3** (101.3 mg, 0.102 mmol) and $HSiEt_3$ (0.16 mL, 1.0 mmol) were dissolved in CH_2Cl_2 (5 mL), and the mixture was stirred at room temperature for 20 h. During this period, the color of the solution changed from orange to red-orange. Addition of hexane to the concentrated solution gave complex **7a** as a dark red crystalline solid (89.3 mg, 0.093 mmol, 92%). ^{1}H NMR (CD_2Cl_2): δ −16.96 (s, 1H, Ir−*H*), 1.05, 1.23 (d, 6H each, J = 6.8 Hz, SCH*Me*$_2$), 2.15 (s, 30H, Cp*), 2.01, 2.94 (sep, 1H each, J = 6.8 Hz, SC*H*Me$_2$). Anal. Calcd for $C_{27}H_{45}F_3Ir_2O_3S_3$: C, 33.95; H, 4.75. Found: C, 33.94; H, 4.73. The corresponding [BF_4]$^-$ salt **7b**, which was used for crystallographic study, was obtained as orange crystals by anion metathesis of **7a** with $NaBF_4$ in THF and recrystallization from CH_2ClCH_2Cl/hexane.

Preparation of [Cp*Ru(μ-PhNO)(μ-SPr^i)$_2$RuCp*][OTf] (8). To a solution of complex **4** (100.3 mg, 0.130 mmol) in THF (5 mL) was added PhNO (36.1 mg, 0.327 mmol), and the mixture was stirred at room temperature for 19 h. The color of the solution changed from dark brown to dark red-brown. Quantitative GLC analysis of the reaction mixture indicated that 0.080 mmol of azoxybenzene was formed. The solid obtained by evaporation of the solvent under reduced pressure was dissolved in THF/benzene (1:1) and loaded on an alumina column. The column was first washed with THF/benzene (1:1), and then the dark brown band that eluted with acetone was collected. The eluate was evaporated under reduced pressure, and the residue was recrystallized from acetone/hexane to give complex **8** as dark brown

(7) Cameron, M.; Gowenlock, B. G.; Vasapollo, G. *Chem. Soc. Rev.* **1990**, *19*, 355−379.
(8) (a) Mansuy, D.; Battioni, P.; Chottard, J.-C.; Riche, C.; Chiaroni, A. *J. Am. Chem. Soc.* **1983**, *105*, 455−463. (b) Hoard, D. W.; Sharp, P. R. *Inorg. Chem.* **1993**, *32*, 612−620.
(9) (a) Cenini, S.; Pizzotti, M.; Crotti, C. In *Aspects of Homogeneous Catalysis*; Ugo, R., Ed.; Reidel: Dordrecht, 1988; Vol. 6, pp 97−198. (b) Ragaini, F.; Cenini, S. *J. Mol. Catal. A: Chem.* **1996**, *109*, 1−25. (c) Skoog, S. J.; Gladfelter, W. L. *J. Am. Chem. Soc.* **1997**, *119*, 11049−11060. (d) Paul, F.; Fischer, J.; Ochsenbein, P.; Osborn, J. A. *Organometallics* **1998**, *17*, 2199−2206.

crystals (98.2 mg, 0.112 mmol, 86%). Anal. Calcd for $C_{33}H_{49}F_3NO_4Ru_2S_3$: C, 45.09; H, 5.62; N, 1.59. Found: C, 45.37; H, 5.73; N, 1.69.

Preparation of [Cp*Rh(μ-PhNO)(μ-SPr^i)$_2$RhCp*][OTf] (9a) and [Cp*Rh(μ-PhNO)(μ-SPr^i)$_2$RhCp*][BPh$_4$] (9b). To a solution of complex **6a** (100.4 mg, 0.129 mmol) in THF (5 mL) was added PhNO (35.6 mg, 0.322 mmol), and the mixture was allowed to reflux for 4 h. The color of the solution changed from dark red-purple to dark brown. Quantitative GLC analysis of the reaction mixture indicated that 0.090 mmol of azoxybenzene was formed. The solid obtained by evaporation of the solvent under reduced pressure was dissolved in acetone/hexane (1:1) and loaded on an alumina column. The first band eluted with acetone/hexane (1:1) was discarded, and the second brown band that eluted with the same solvent was collected. The eluate was evaporated under reduced pressure, and the residue was recrystallized from acetone/hexane to give complex **9a** as a dark brown crystalline solid (63.5 mg, 0.072 mmol, 56%). Anal. Calcd for $C_{33}H_{49}F_3NO_4Rh_2S_3$: C, 44.90; H, 5.59; N, 1.59. Found: C, 45.00; H, 5.72; N, 1.58. The corresponding $[BPh_4]^-$ salt **9b**, which was used for crystallographic study, was obtained as dark brown crystals by anion metathesis of **9a** with $NaBPh_4$ in THF and recrystallization from CH_2Cl_2/ether.

Preparation of [Cp*Ir(μ-PhNO)(μ-SPr^i)$_2$IrCp*][OTf] (10a) and [Cp*Ir(μ-PhNO)(μ-SPr^i)$_2$IrCp*][BPh$_4$] (10b). To a solution of **7a** (101.1 mg, 0.106 mmol) in THF (5 mL) was added PhNO (30.8 mg, 0.279 mmol), and the mixture was allowed to reflux for 4 h. The color of the solution changed from orange to dark brown. Quantitative GLC analysis of the reaction mixture indicated that 0.049 mmol of azoxybenzene was formed. The solid obtained by evaporation of the solvent under reduced pressure was dissolved in acetone and loaded on an alumina column. The column was washed with hexane, and the red-brown band that eluted with acetone was collected. The eluate was evaporated under reduced pressure, and the residue was recrystallized from acetone/hexane to give complex **10a** as a dark brown crystalline solid (101.4 mg, 0.096 mmol, 90%). Anal. Calcd for $C_{33}H_{49}F_3Ir_2NO_4S_3$: C, 37.34; H, 4.65; N, 1.32. Found: C, 37.14; H, 4.69; N, 1.31. The corresponding $[BPh_4]^-$ salt **10b**, which was used for crystallographic study, was obtained as dark brown crystals by anion metathesis of **10a** with $NaBPh_4$ in THF and recrystallization from CH_2Cl_2/ether.

Preparation of [Cp*$_3$Rh$_3$(μ-Cl)$_2$(μ$_3$-S)(μ-SPr^i)][OTf]·0.5(CH$_3$COCH$_3$) (11a·0.5(CH$_3$COCH$_3$)) and [Cp*$_3$Rh$_3$(μ-Cl)$_2$(μ$_3$-S)(μ-SPr^i)][BPh$_4$]·0.5(CH$_3$COCH$_3$) (11b·0.5(CH$_3$COCH$_3$)). To a solution of **2** (152.7 mg, 0.188 mmol) in THF (10 mL) was added PhNO (101.0 mg, 0.943 mmol), and the mixture was allowed to reflux for 24 h. The color of the solution changed from red to dark red-brown. The solid obtained by evaporation of the solvent under reduced pressure was dissolved in acetone and loaded on an alumina column. The column was washed with benzene, and then the red-brown band that eluted with acetone was collected. The eluate was evaporated under reduced pressure, and the residue was washed with ether. Recrystallization of the residual solid from acetone/hexane gave **11a**·0.5(CH_3COCH_3) as a dark brown crystalline solid (93.7 mg, 0.088 mmol, 70%). ^{1}H NMR ($CDCl_3$): δ 1.16 (d, 6H, J = 6.9 Hz, SCH*Me*$_2$), 1.54 (s, 15H, Cp*), 1.55 (s, 30H, Cp*), 3.65 (sep, 1H, J = 6.9 Hz, SC*H*Me$_2$). Anal. Calcd for $C_{35.5}H_{55}Cl_2F_3O_{3.5}Rh_3S_3$: C, 39.83; H, 5.18; Cl, 6.62; S, 8.99. Found: C, 40.02; H, 5.25; Cl, 6.82; S, 9.07. The corresponding $[BPh_4]^-$ salt **11b**·0.5(CH_3COCH_3), which was used for crystallographic study, was obtained as dark red crystals by anion metathesis of **11a**·0.5(CH_3COCH_3) with $NaBPh_4$ in THF and recrystallization from acetone/hexane.

Reaction of 6a with Et$_3$N. To a solution of **6a** (102.1 mg, 0.131 mmol) in THF (5 mL) was added Et_3N (0.18 mL, 1.3 mmol), and the mixture was stirred at 50 °C for 15 h. The color of the solution changed from dark red-purple to dark blue-purple. The solvent was removed in vacuo, and the resulting solid was extracted with hexane. The extract was dried up to give [Cp*Rh(μ-SPr^i)]$_2$ as a dark brown powder (69.2 mg, 0.110 mmol, 84%). In benzene solution, this complex exists as an equilibrium mixture of syn and anti isomers with respect to the SPr^i groups. ^{1}H NMR (C_6D_6): anti isomer; δ 1.33, 1.37 (d, 6H each, J = 6.8 Hz, SCH*Me*$_2$), 1.92 (s, 30H, Cp*), 2.25, 2.47 (sep, 1H each, J = 6.8 Hz, SC*H*Me$_2$), syn isomer; δ 1.41 (d, 12H, J = 6.8 Hz, SCH*Me*$_2$), 1.92 (s, 30H, Cp*), 2.25 (sep, 2H, J = 6.8 Hz, SC*H*Me$_2$). Anal. Calcd for $C_{26}H_{44}Rh_2S_2$: C, 49.84; H, 7.08. Found: C, 49.46; H, 7.05.

Reaction of 7a with Et$_3$N. To a solution of **7a** (199.0 mg, 0.208 mmol) in THF (10 mL) was added Et_3N (0.29 mL, 2.1 mmol), and the mixture was stirred at 50 °C for 15 h. The color of the solution changed from red-orange to dark red-brown. The solvent was removed in vacuo, and the resulting solid was extracted with hexane. The extract was dried up to give [Cp*Ir(μ-SPr^i)]$_2$ as a brown powder (59.7 mg, 0.074 mmol, 36%), which was identified by comparison of the ^{1}H NMR spectrum with that of an authentic sample.[4]

X-ray Crystallographic Studies. Single crystals of **5**, **6b**·0.5(CH_2Cl_2), **7b**, **8**, **9b**, **10b**, and **11b**·0.5(CH_3COCH_3) were sealed in glass capillaries under an argon atmosphere and used for data collection. Diffraction data were collected on a Rigaku AFC7R four-circle automated diffractometer with graphite-monochromatized Mo Kα radiation (λ = 0.710 69 Å) at room temperature, using the $\omega-2\theta$ scan technique for **5**, **6b**·0.5(CH_2Cl_2), **7b**, **8**, **9b**, and **10b** and the ω scan technique for **11b**·0.5(CH_3COCH_3). The orientation matrixes and unit cell parameters were determined by least-squares refinement of 25 (for **5**, **6b**·0.5(CH_2Cl_2), **7b**, **8**, **9b**, and **10b**) or 24 (for **11b**·0.5(CH_3COCH_3)) machine-centered reflections with 38.9° < 2θ < 39.6° for **5**, 38.8° < 2θ < 40.0° for **6b**·0.5(CH_2Cl_2), 32.8° < 2θ < 38.0° for **7b**, 28.4° < 2θ < 38.9° for **8**, 23.6° < 2θ < 27.9° for **9b**, 36.4° < 2θ < 39.9° for **10b**, and 27.3° < 2θ < 37.5° for **11b**·0.5(CH_3COCH_3). Intensity data were corrected for Lorentz and polarization effects and for absorption (empirical, ψ scans). For crystals of **6b**·0.5(CH_2Cl_2), **8**, **9b**, **10b**, and **11b**·0.5(CH_3COCH_3), no significant decay was observed for three standard reflections monitored every 150 reflections during the data collection. For compounds **5** and **7b**, a slight decay (**5**, 1.56%; **7b**, 2.56%) was observed during the data collection, and a correction for decay was applied in each case.

The structure solution and refinements were carried out by using the teXsan crystallographic software package.[11] The positions of the non-hydrogen atoms were determined by Patterson methods (DIRDIF PATTY[12]) and subsequent Fourier syntheses. All non-hydrogen atoms were refined by full-matrix least-squares techniques with anisotropic thermal parameters, except for the carbon atom of $[OTf]^-$ anion in **5** and the carbon and oxygen atoms of the acetone molecule in **11b**·0.5(CH_3COCH_3) where isotropic parameters were used. The CH_2Cl_2 molecule in **6b**·0.5(CH_2Cl_2) was found to be located on the center of symmetry, and the carbon atom of this CH_2Cl_2 molecule was refined with an atom multiplicity of 0.5. Hydrogen atoms, except for those of the CH_2Cl_2 molecule in **6b**·0.5(CH_2Cl_2), the acetone molecule in **11b**·0.5(CH_3COCH_3), and the hydrido ligands in **5**, **6b**·0.5(CH_2Cl_2), and **7b**, were placed at the calculated positions (d_{C-H} = 0.95 Å), while the positions of the hydrido ligands were found in the final difference Fourier maps. These hydrogen atoms were included with fixed isotropic parameters. Details of the X-ray diffraction study are summarized in Tables 1 and 2.

Results and Discussion

Synthesis of the Ruthenium Hydrido Complex [Cp*RuH(μ-SPr^i)$_2$RuCp*]$^+$. When complex **1** was allowed to react with $HSiEt_3$ in CH_2Cl_2 at room temperature, the dinuclear hydrido complex [Cp*RuH(μ-SPr^i)$_2$RuCp*][OTf] (**4**) was obtained in high yield (eq 1). It has been known that hydrosilanes behave as an effective hydrogen source for the syntheses of hydrido complexes.[13] The electroconductivity of **4** in CH_2Cl_2 (72.5 S

(10) White, C.; Yates, A.; Maitlis, P. M. *Inorg. Synth.* **1992**, *29*, 228−234.
(11) *teXsan: Crystal Structure Analysis Package*; Molecular Structure Corp.: The Woodlands, TX, 1985 and 1992.
(12) PATTY: Beurskens, P. T.; Admiraal, G.; Beurskens, G.; Bosman, W. P.; Garcia-Granda, S.; Gould, R. O.; Smits, J. M. M.; Smykalla, C. *The DIRDIF program system*; Technical Report of the Crystallography Laboratory, University of Nijmegen: Nijmegen, The Netherlands, 1992.

Table 1. X-ray Crystallographic Data for **5**, **6b**·0.5(CH_2Cl_2), **7b**, and **8**

	5	**6b**·0.5(CH_2Cl_2)	**7b**	**8**
chemical formula	$C_{29}H_{48}F_3NO_3Ru_2S_3$	$C_{50.5}H_{66}BClRh_2S_2$	$C_{26}H_{45}BF_4Ir_2S_2$	$C_{33}H_{49}F_3NO_4Ru_2S_3$
formula wt	814.02	989.27	893.01	879.07
space group	$P\bar{1}$	$P2_1/n$	$P2_1/n$	$P2_1/c$
a, Å	9.747(1)	16.279(2)	9.334(3)	14.802(3)
b, Å	12.578(1)	15.332(2)	21.871(1)	12.929(4)
c, Å	15.049(2)	19.936(2)	15.644(3)	19.735(3)
α, deg	104.385(8)			
β, deg	94.942(8)	104.188(9)	104.28(2)	95.48(1)
γ, deg	90.446(8)			
V, Å^3	1779.6(7)	4824(1)	3095(1)	3759(1)
Z	2	4	4	4
ρ_{calcd}, g cm^{-3}	1.519	1.362	1.916	1.553
μ(Mo Kα), cm^{-1}	10.69	8.57	87.87	10.21
R^a	0.047	0.040	0.037	0.042
$R_w{}^b$	0.047	0.026	0.026	0.030

$^a R = \sum||F_o| - |F_c||/\sum|F_o|$. $^b R_w = [\sum w(|F_o| - |F_c|)^2/\sum wF_o^2]^{1/2}$, $w = 1/\sigma^2(F_o)$.

Table 2. X-ray Crystallographic Data for **9b**, **10b**, and **11b**·0.5(CH_3COCH_3)

	9b	**10b**	**11b**·0.5(CH_3COCH_3)
chemical formula	$C_{56}H_{69}BNORh_2S_2$	$C_{56}H_{69}BIr_2NOS_2$	$C_{58.5}H_{75}BCl_2O_{0.5}Rh_3S_2$
formula wt	1052.91	1231.54	1240.79
space group	$P2_1/n$	$P2_1/n$	$P\bar{1}$
a, Å	11.045(3)	11.031(5)	9.0280(8)
b, Å	24.286(3)	24.316(5)	17.032(2)
c, Å	19.249(3)	19.226(7)	37.455(4)
α, deg			98.453(8)
β, deg	90.94(2)	90.91(4)	93.899(7)
γ, deg			91.642(8)
V, Å^3	5162(1)	5156(2)	5679(3)
Z	4	4	4
ρ_{calcd}, g cm^{-1}	1.355	1.586	1.451
μ(Mo Kα), cm^{-1}	7.57	52.90	10.64
R^a	0.047	0.038	0.047
$R_w{}^b$	0.033	0.026	0.029

$^a R = \sum||F_o| - |F_c||/\sum|F_o|$. $^b R_w = [\sum w(|F_o| - |F_c|)^2/\sum wF_o^2]^{1/2}$, $w = 1/\sigma^2(F_o)$.

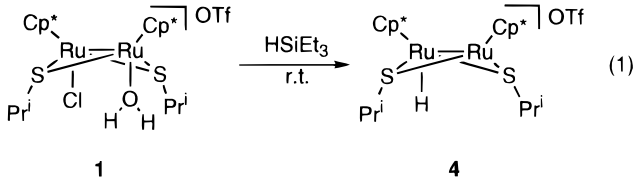

1 **4** (1)

cm^2 mol^{-1}) clearly indicated its monocationic nature in solution. In the IR spectrum, complex **4** exhibited a ν_{Ru-H} band at 1968 cm^{-1} in the solid state (KBr) and at 1962 cm^{-1} in CH_2Cl_2 solution, which is diagnostic of a terminally bound hydrido ligand. On the other hand, the ^{1}H NMR spectrum of **4** at room temperature showed only one Cp* signal (δ 1.75 (s)) and one set of Pr^i signals (δ 0.99 (d), 3.31 (sep)) in addition to a Ru−H resonance at δ −13.56. At −60 °C, the Me resonance of the Pr^i group appeared as a broad peak, while other signals displayed no notable temperature dependence. On the basis of these spectral properties, we consider that the dinuclear core of complex **4** is, at least in the solution state, composed of a formal 18-electron Ru(III) center with a terminal hydrido ligand and an apparent 16-electron Ru(III) center bridged by two mutually syn SPr^i ligands, and the hydrido ligand undergoes facile migration between the two ruthenium atoms over the temperature range of 20 to −60 °C (eq 2). However, we cannot rule out the solid-state structure with a coordinated [OTf]$^-$ anion. A similar fluxional behavior of a chloro ligand was observed for related coordinatively unsaturated diruthenium complexes [Cp*RuCl(μ-EFc)$_2$RuCp*][OTf] (E = S, Se, Te; Fc = ferrocenyl).[14]

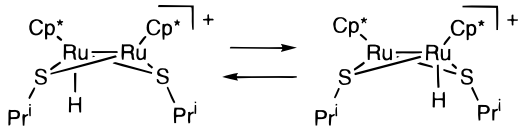

(2)

The acetonitrile derivative [Cp*RuH(μ-SPr^i)$_2$Ru(NCMe)Cp*][OTf] (**5**) was synthesized by reacting **4** with acetonitrile (eq 3), and its molecular structure was established by X-ray analysis.

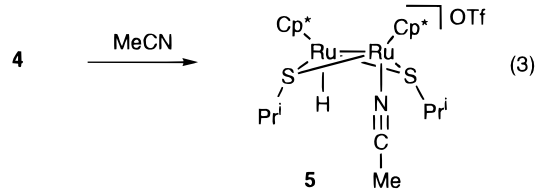

(3)

The structure of the cationic part is given in Figure 1, and selected bond distances and angles are in Table 3. The position of the hydrido ligand was located in the final difference Fourier map. The complex comprises a thiolato-bridged diruthenium core where the intramolecular distance between the ruthenium

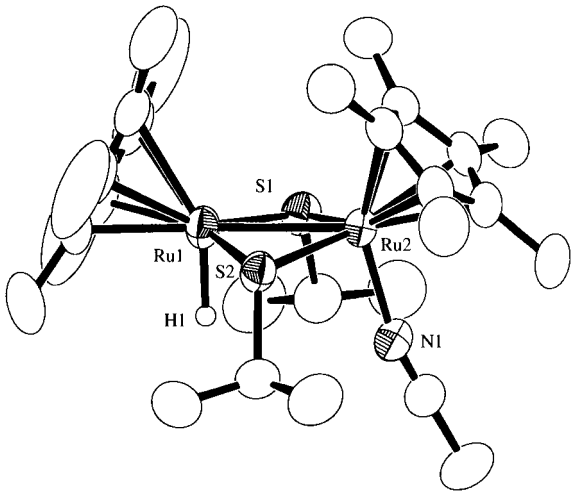

Figure 1. Structure of the cationic part in **5**. Hydrogen atoms, except for the hydrido ligand, are omitted for clarity.

Table 3. Selected Interatomic Distances and Angles in **5**

Distances (Å)			
Ru(1)−Ru(2)	2.8099(7)	Ru(1)−S(1)	2.269(2)
Ru(1)−S(2)	2.268(2)	Ru(1)−H(1)	1.59
Ru(2)−S(1)	2.337(2)	Ru(2)−S(2)	2.330(2)
Ru(2)−N(1)	2.066(5)		
Angles (deg)			
Ru(2)−Ru(1)−S(1)	53.51(4)	Ru(2)−Ru(1)−S(2)	53.33(4)
Ru(2)−Ru(1)−H(1)	91.6	S(1)−Ru(1)−S(2)	105.11(5)
Ru(1)−Ru(2)−S(1)	51.33(4)	Ru(1)−Ru(2)−S(2)	51.34(4)
Ru(1)−Ru(2)−N(1)	102.7(1)	S(1)−Ru(2)−S(2)	101.06(5)
Ru(1)−S(1)−Ru(2)	75.17(5)	Ru(1)−S(2)−Ru(2)	75.34(5)

(13) For example: Fernandez, M. J.; Maitlis, P. M. *Organometallics* **1983**, *2*, 164−165.

(14) Matsuzaka, H.; Qü, J.-P.; Ogino, T.; Nishio, M.; Nishibayashi, Y.; Ishii, Y.; Uemura, S.; Hidai, M. *J. Chem. Soc., Dalton Trans.* **1996**, 4307−4312.

atoms (2.8099(7) Å) corresponds to a Ru−Ru single bond.[2d,3e,14] The acetonitrile and hydrido ligands are coordinated in mutually cis configuration to the two respective ruthenium centers, and the SPr^i groups adopt a syn arrangement. The Ru_2S_2 ring is puckered slightly toward the hydrido and acetonitrile ligands with the dihedral angle of 162.8° around the Ru−Ru axis. The IR (KBr) and ^1H NMR (−40 °C) spectra of complex **5** showed a ν_{Ru-H} band at 1943 cm^{-1} and a hydrido resonance at δ −15.51, respectively, both of which are comparable to those observed with complex **4**, although the Pr^i and Cp* signals of **5** in the ^1H NMR spectrum coalesced at room temperature into broad peaks at δ 1.3−2.3.

Synthesis of the Rhodium and Iridium Hydrido Complexes [Cp*M(μ-H)(μ-SPr^i)$_2$MCp*]$^+$. The cationic dirhodium and diiridium complexes **2** and **3**, which were synthesized by treating the dichloro complexes [Cp*MCl(μ-SPr^i)$_2$MClCp*] (M = Rh, Ir) with AgOTf, also reacted with $HSiEt_3$ at room temperature to give the cationic hydrido complexes [Cp*M(μ-H)(μ-SPr^i)$_2$MCp*][OTf] (**6a**, M = Rh; **7a**, M = Ir) in high yields (eq 4). The ^1H NMR spectrum of **6a** exhibited a triplet

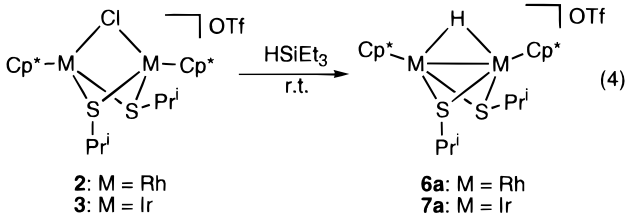

signal at δ −13.40 attributable to the hydrido ligand (J_{Rh-H} = 23.2 Hz), demonstrating that the hydrido ligand in **6a** takes a bridging coordination mode in contrast to that in **4**. In accord with the ^1H NMR spectra, complex **6a** showed no IR absorption attributable to a terminal M−H stretching in the range 1500−2200 cm^{-1}. Furthermore, the ^1H NMR signal of the Cp* protons appeared as a singlet at δ 1.98, while those of the SPr^i protons as two sets of doublet (δ 1.06, 1.22) and septet (δ 2.07, 2.70) with the same intensities. These spectral data are consistent with a dirhodium core structure symmetrically bridged by one hydrido and two thiolato ligands, where the SPr^i groups are arranged in an anti configuration. Complex **7a** showed similar IR and ^1H NMR features, except that the hydrido signal of **7a** appeared as a singlet at δ −16.96, indicating that complex **7a** also has a symmetric dinuclear core bridged by one hydrido and two SPr^i ligands with anti stereochemistry. It should be noted that the dinuclear cation in **7a** is the same as that of [Cp*Ir(μ-H)(μ-SPr^i)$_2$IrCp*][$OCOCF_3$], which we previously synthesized from [Cp*Ir(μ-SPr^i)$_2$IrCp*] by protonation with CF_3COOH.[4] From a practical point of view, the present reaction using $HSiEt_3$ provides a more convenient method to obtain the dinuclear hydrido complex. On the other hand, treatment of **6a** and **7a** with NEt_3 in THF at 50 °C produced [Cp*Rh(μ-SPr^i)$_2$RhCp*] and [Cp*Ir(μ-SPr^i)$_2$IrCp*], respectively, revealing the acidic nature of these hydride complexes. The ruthenium complex **4**, however, failed to react with NEt_3 at this temperature.

The solid-state structures of these dirhodium and diiridium cations were confirmed by crystallographic analysis of [Cp*Rh(μ-H)(μ-SPr^i)$_2$RhCp*][BPh_4]·0.5(CH_2Cl_2) (**6b**·0.5(CH_2Cl_2)), the [BPh_4]$^-$ analogue of **6a**, and [Cp*Ir(μ-H)(μ-SPr^i)$_2$IrCp*][BF_4] (**7b**), the [BF_4]$^-$ analogue of **7a**. ORTEP drawings of the cationic parts in **6b** and **7b** are illustrated in Figure 2, and selected bond distances and angles are contained in Table 4. The positions of the bridging hydrido ligands were located unequivocally in the respective final difference Fourier maps.

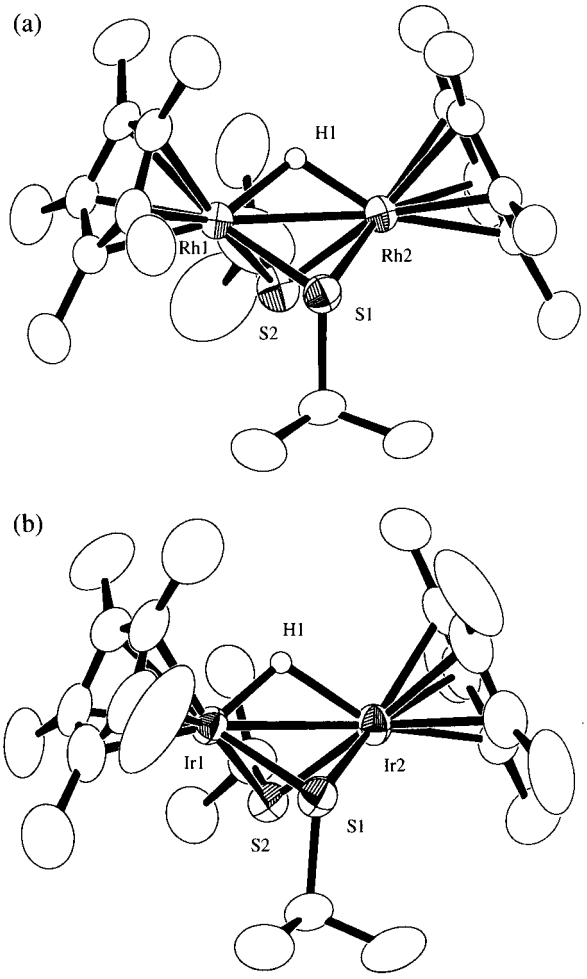

Figure 2. Structures of the cationic parts in **6b**·0.5(CH_2Cl_2) (a) and **7b** (b). Hydrogen atoms, except for the hydrido ligand, are omitted for clarity.

Table 4. Selected Interatomic Distances and Angles in **6b**·0.5(CH_2Cl_2) and **7b**

	6b·0.5(CH_2Cl_2) (M = Rh)	**7b** (M = Ir)
	Distances (Å)	
M(1)−M(2)	2.7375(5)	2.7720(5)
M(1)−S(1)	2.344(1)	2.3628(5)
M(1)−S(2)	2.363(1)	2.3863(7)
M(1)−H(1)	1.70	1.58
M(2)−S(1)	2.345(1)	2.3565(3)
M(2)−S(2)	2.363(1)	2.3622(3)
M(2)−H(1)	1.65	1.86
	Angles (deg)	
M(2)−M(1)−S(1)	54.29(3)	53.924(9)
M(2)−M(1)−S(2)	54.59(3)	53.880(8)
S(1)−M(1)−S(2)	79.30(4)	77.99(1)
M(1)−M(2)−S(1)	54.26(3)	54.13(2)
M(1)−M(2)−S(2)	54.61(3)	54.69(2)
S(1)−M(2)−S(2)	79.29(4)	78.59(2)
M(1)−S(1)−M(2)	71.44(3)	71.94(2)
M(1)−S(2)−M(2)	70.80(3)	71.43(2)

The structures of **6b** and **7b** are closely related to each other. In full agreement with the spectral data, they have triply bridged dinuclear cores where the distances between the metal centers (Rh(1)−Rh(2), 2.7375(5) Å; Ir(1)−Ir(2), 2.7720(5) Å) as well as the M−H−M angles (Rh(1)−H(1)−Rh(2), 109.9°; Ir(1)−H(1)−Ir(2), 107.1°) suggest that these complexes have substantial metal−metal bonding character within the M−H−M three-center two-electron bonds.[15−17] In each case, the SPr^i

ligands take an anti configuration, and the M_2S_2 core strongly puckers away from the bridging hydrido ligand with the dihedral angle of 102.3° for **6b** and 103.3° for **7b** around the metal−metal axis. Related cationic dinuclear cores with hydrido and thiolato bridges have been reported for $[Cp^*_2Ir_2Cl_2(\mu\text{-H})(\mu\text{-SR})]$ (R = Bu, $C_6H_4CH_2CH_3$),[17] $[Ir_2(\mu\text{-H})(H)_2(\mu\text{-SH})(\mu\text{-SR})(PPh_3)_4]^+$ (R = H, Pr^i),[18] and $[Ir_2(\mu\text{-H})(H)_2(\mu\text{-SBu}^t)_2(CO)_2(PR_3)_2]^+$ (R = Me, Ph, OMe).[19] It is worth mentioning that the diruthenium complex **4** and the dirhodium and diiridium complexes **6** and **7** have significantly different core structures with respect to the coordination mode of the hydrido ligand and the stereochemistry of SPr^i ligands, although the composition of the ligands in these complexes is the same. In addition, the difference in the core structure is reflected in their reaction with acetonitrile. Thus, the terminal hydrido complex **4** underwent facile reaction with acetonitrile to give **5** as mentioned above, but the bridging hydrido complexes **6** and **7** did not react with this nitrile under the same conditions.

Reactions of the Dinuclear Hydrido Complexes 4, 6a, and 7a with Nitrosobenzene. The diruthenium complex **4** reacted with an excess amount of nitrosobenzene at room temperature to form the cationic nitrosobenzene complex $[Cp^*Ru(\mu\text{-PhNO})(\mu\text{-SPr}^i)_2RuCp^*][OTf]$ (**8**). The GLC and GC−MS analyses of the reaction mixture indicated the concomitant formation of azoxybenzene (0.6 mol per **4**). The dirhodium complex **6a** and diiridium complex **7a** failed to react with nitrosobenzene at room temperature, but in refluxing THF they were smoothly transformed into the corresponding cationic nitrosobenzene complexes $[Cp^*Rh(\mu\text{-PhNO})(\mu\text{-SPr}^i)_2RhCp^*][OTf]$ (**9a**) and $[Cp^*Ir(\mu\text{-PhNO})(\mu\text{-SPr}^i)_2IrCp^*][OTf]$ (**10a**), respectively. Formation of azoxybenzene (0.70 mol per **6a**, 0.46 mol per **7a**) was also confirmed by means of GLC. In all cases, H_2 was not detected in the gaseous phase. On the basis of these observations, we propose that the total reaction follows the stoichiometry shown in eq 5 irrespective of the metal elements of the hydrido

$$\underset{\textbf{4, 6a, 7a}}{[Cp^*MH(\mu\text{-SPr}^i)_2MCp^*][OTf]} + 2\ PhNO \longrightarrow 1/2\ PhN(O)NPh + 1/2\ H_2O + [Cp^*M(\mu\text{-PhNO})(\mu\text{-SPr}^i)_2MCp^*][OTf] \quad (5)$$

8: M = Ru
9a: M = Rh
10a: M = Ir

complexes. In the reactions of complexes **4** and **6a**, the yield of azoxybenzene was somewhat higher than that expected from eq 5 (0.5 mol per **4**, **6a**, or **7a**), but we consider that azoxybenzene was also formed through side reactions, such as oxygenation of the bridging thiolato ligands by nitrosobenzene. Although details of the reaction mechanism are unclear, formation of azoxybenzene from reactions of nitrosobenzene with metal complexes has been well-documented.[20]

Table 5. Selected Interatomic Distances and Angles in **8**, **9b**, and **10b**

	8 (M = Ru)	**9b** (M = Rh)	**10b** (M = Ir)
	Distances (Å)		
M(1)−M(2)	2.7057(8)	3.3648(9)	3.421(1)
M(1)−S(1)	2.312(1)	2.359(2)	2.362(2)
M(1)−S(2)	2.303(2)	2.379(2)	2.385(3)
M(1)−O(1)	2.091(3)	2.054(5)	2.066(6)
M(2)−S(1)	2.314(2)	2.373(2)	2.373(3)
M(2)−S(2)	2.316(1)	2.374(2)	2.373(3)
M(2)−N(1)	2.093(4)	2.110(6)	2.092(7)
O(1)−N(1)	1.353(5)	1.333(6)	1.339(8)
N(1)−C(21)	1.391(6)	1.391(8)	1.40(1)
	Angles (deg)		
M(2)−M(1)−O(1)	72.19(10)		
S(1)−M(1)−S(2)	108.29(5)	80.23(7)	78.54(8)
S(1)−M(1)−O(1)	83.2(1)	85.0(1)	83.6(2)
S(2)−M(1)−O(1)	81.9(1)	84.2(1)	82.6(2)
M(1)−M(2)−N(1)	70.0(1)		
S(1)−M(2)−S(2)	107.78(5)	80.05(7)	78.55(9)
S(1)−M(2)−N(1)	80.2(1)	84.6(2)	84.0(2)
S(2)−M(2)−N(1)	82.2(1)	84.2(2)	82.9(2)
M(1)−S(1)−M(2)	71.59(4)	90.64(7)	92.54(9)
M(1)−S(2)−M(2)	71.71(4)	90.14(7)	91.96(9)
M(1)−O(1)−N(1)	106.7(3)	121.1(4)	121.7(5)
M(2)−N(1)−O(1)	110.9(3)	117.3(4)	118.4(6)
M(2)−N(1)−C(21)	136.3(4)	132.7(5)	131.8(6)
O(1)−N(1)−C(21)	112.8(4)	109.3(6)	109.5(7)

The nitrosobenzene complexes obtained herein are paramagnetic, and their ^{1}H NMR measurements were not informative. However, their structures were unambiguously determined by X-ray diffraction study of **8**, $[Cp^*Rh(\mu\text{-PhNO})(\mu\text{-SPr}^i)_2RhCp^*][BPh_4]$ (**9b**), the $[BPh_4]^-$ analogue of **9a**, and $[Cp^*Ir(\mu\text{-PhNO})(\mu\text{-SPr}^i)_2IrCp^*][BPh_4]$ (**10b**), the $[BPh_4]^-$ analogue of **10a**. ORTEP drawings are depicted in Figure 3, and selected bond distances and angles are listed in Table 5. The dinuclear cores of **8**, **9b**, and **10b** are bridged by two SPr^i ligands with syn stereochemistry and a μ-η^1:η^1-PhNO-*N*,*O* ligand in which the nitrogen and oxygen atoms are coordinated to the two respective metal centers. The Ru−Ru distance at 2.7057(8) Å in **8** corresponds to a metal−metal single bond,[2d,3e,14] while the Rh−Rh separation in **9b** (3.3648(9) Å) and the Ir−Ir separation in **10b** (3.421(1) Å) suggest the absence of bonding interaction between the core metal atoms in **9b** and **10b**. In each complex, the M_2NO ring is almost planar, and the phenyl group is slightly twisted from this plane with the dihedral angle of 15.0° (**8**)−18.1° (**9b**). Interestingly, the Ru_2S_2 ring in complex **8** is nearly planar (the dihedral angle between the Ru_2S units is 172.76°), while complexes **9b** and **10b** take the conformation where the M_2S_2 (M = Rh, Ir) rings are puckered with the dihedral angles between the M_2S planes of 131.98° and 131.94° for **9b** and **10b**, respectively.

Several types of bridging coordination modes have been found for *C*-nitroso compound ligands in multinuclear transition metal complexes,[8b,21−24] where the μ-η^1:η^2-*N*,*O* coordination mode has been observed most commonly.[8b,21] As described above, complexes **8**−**10** are classified as less common μ-η^1:η^1-*N*,*O* complexes.[22,23] The N−O bond distances found in **8** (1.353(5) Å), **9b** (1.333(6) Å), and **10b** (1.339(8) Å) are longer than the N=O double bond distances of free nitrosoarene monomers

(15) (a) Bau, R.; Teller, R. G.; Kirtley, S. W.; Koetzle, T. F. *Acc. Chem. Res.* **1979**, *12*, 176−183. (b) Crabtree, R. H. In *Comprehensive Coordination Chemistry*; Wilkinson, G., Gillard, R. D., McCleverty, J. A., Eds.; Pergamon Press: Oxford, 1987; Vol. 2, pp 689−714.
(16) (a) Churchill, M. R.; Ni, S. W.-Y. *J. Am. Chem. Soc.* **1973**, *95*, 2150−2155. (b) Churchill, M. R.; Julis, S. A. *Inorg. Chem.* **1977**, *16*, 1488−1494. (c) Gilbert, T. M.; Hollander, F. J.; Bergman, R. G. *J. Am. Chem. Soc.* **1985**, *107*, 3508−3516.
(17) Vicic, D. A.; Jones, W. D. *Organometallics* **1997**, *16*, 1912−1919.
(18) Mueting, A. M.; Boyle, P. D.; Wagner, R.; Pignolet, L. H. *Inorg. Chem.* **1988**, *27*, 271−279.
(19) Bonnet, J. J.; Thorez, A.; Maisonnat, A.; Galy, J.; Poilblanc, R. *J. Am. Chem. Soc.* **1979**, *101*, 5940−5948.
(20) For example: (a) Thiyagarajan, B.; Kerr, M. E.; Bruno, J. W. *Inorg. Chem.* **1995**, *34*, 3444−3452. (b) Ragaini, F.; Song, J.-S.; Ramage, D. L. Geoffroy, G. L.; Yap, G. A. P.; Rheingold, A. L. *Organometallics*, **1995**, *14*, 387−400.

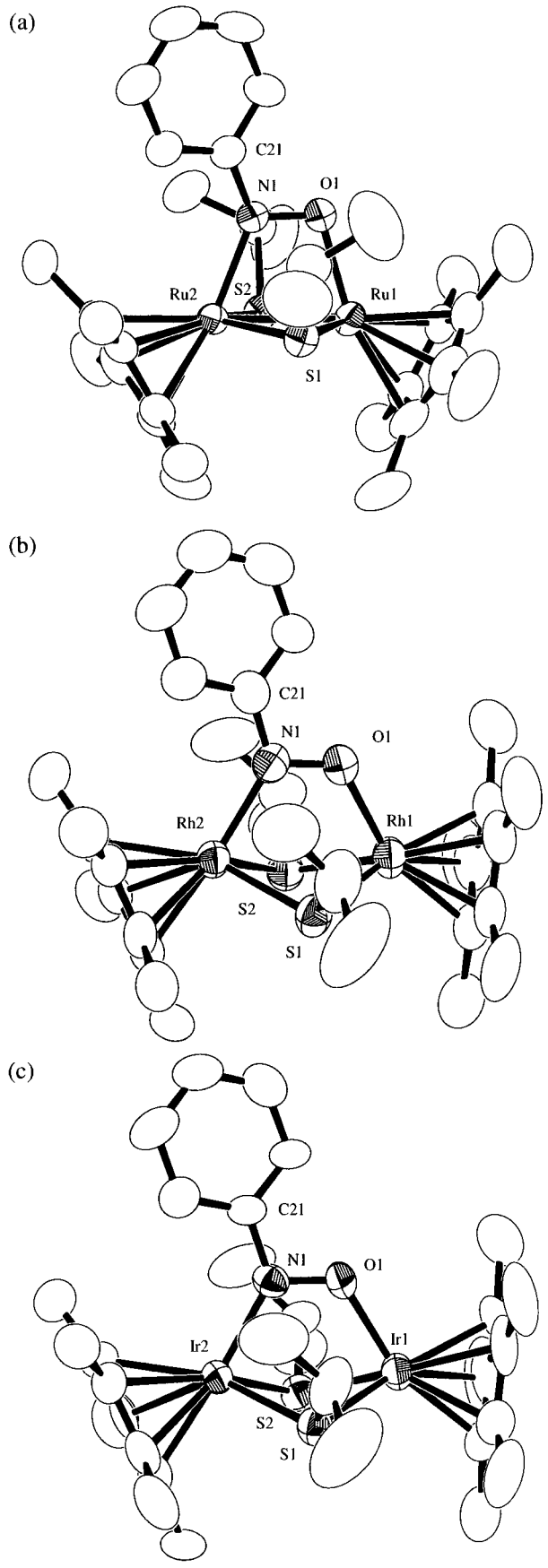

Figure 3. Structures of the cationic parts in **8** (a), **9b** (b), and **10b** (c). Hydrogen atoms are omitted for clarity.

(1.21−1.28 Å)[25] and are comparable to the values reported for the μ-η^1:η^1-*N,O* nitrosoarene ligands in ruthenium clusters [Ru_3(μ-$ONC_{10}H_6O)_2(CO)_8$] (1.30(1), 1.31(1) Å)[22a] and [Ru_3(μ-$NPh)_2$(μ-$PhNO)_2(CO)_7$] (1.334(9) Å)[22b] but are considerably shorter than that described for the nitrosobenzene ligand of this type in [$(Me_3P)_2Pt$(μ-η^1:η^1-PhNO)(μ-η^1-PhNO)Pt(PhNO)(PMe_3)] (1.433(15) Å).[22c] It should be noted that the μ-η^1:η^1-PhNO ligand in the last complex is regarded as a dianionic ligand with an N−O single bond. Judging from the N−O bond distances, the nitrosobenzene ligands in complexes **8**, **9b**, and **10b** retain some N═O double bond character.

Chart 1

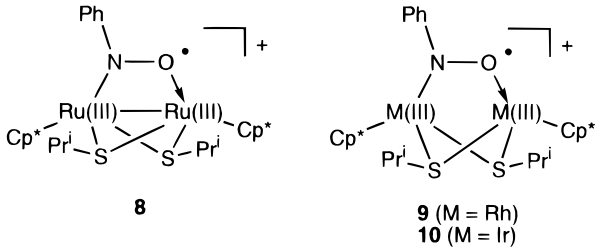

8 **9** (M = Rh) **10** (M = Ir)

To gain further insight into the structures of the complexes **8**−**10**, their ESR spectra were measured. In CH_2Cl_2 at 20 °C, complexes **8** and **9a** showed a triplet signal revealing a hyperfine interaction with the nitroso nitrogen atom (**8**, g_{iso} = 1.998, a_{iso} = 14.2 G; **9a**, g_{iso} = 2.010, a_{iso} = 13.6 G), while complex **10a** exhibited a singlet signal (g_{iso} = 2.023). No hyperfine interaction with the rhodium or hydrogen atoms was observed. These data imply that, at least in complexes **8** and **9a**, the unpaired electron is mainly located on the nitrosobenzene ligand. For several paramagnetic nitrosoarene complexes, structures with an unpaired electron located on or highly delocalized onto the nitrosoarene ligand have been proposed.[26] Furthermore, when the unpaired electron is accommodated in the nitrosobenzene ligand (Chart 1), the total electron counts for the dimetallic cores of complexes **8**, **9**, and **10** are 34e$^-$, 36e$^-$, and 36e$^-$, respectively, which are consistent with the above-mentioned molecular structures with a Ru−Ru single bond in **8** and no metal−metal bonding interaction in **9b** and **10b**.

In the cyclic voltammograms, each of complexes **8**, **9a**, and **10a** in CH_2Cl_2/0.1 M [Bu_4N][BF_4] showed a reversible oxidation wave ($E_{1/2}$: **8**, 0.66 V; **9a**, 0.45 V; **10a**, 0.45 V vs SCE). Thus, the redox potentials for the [Cp*M(μ-PhNO)(μ-$SPr^i)_2$MCp*]$^{2+,+}$ couples are relatively close to each other. In sharp contrast, the related dichloro complexes [Cp*MCl(μ-$SPr^i)_2$MClCp*] (M =

(21) (a) Barrow, M. J.; Mills, O. S. *J. Chem. Soc. A* **1971**, 864−868. (b) Otsuka, S.; Aotani, Y.; Tatsuno, Y.; Yoshida, T. *Inorg. Chem.* **1976**, *15*, 656−660. (c) Middleton, A. R.; Wilkinson, G. *J. Chem. Soc., Dalton Trans.* **1981**, 1898−1905. (d) Stella, S.; Floriani, C.; Chiesi-Villa, A.; Guastini, C. *J. Chem. Soc., Dalton Trans.* **1988**, 545−547. (e) Ang, H. G.; Kwik, W. L.; Ong, K. K. *J. Fluorine Chem.* **1993**, *60*, 43−48.

(22) (a) Lee, K. K. H.; Wong, W. T. *J. Chem. Soc., Dalton Trans.* **1996**, 3911−3912. (b) Lee, K. K.-H.; Wong, W.-T. *J. Chem. Soc., Dalton Trans.* **1997**, 2987−2995. (c) Packett, D. L.; Trogler, W. C.; Rheingold, A. L. *Inorg. Chem.* **1987**, *26*, 4308−4309.

(23) The recently reported Pt−Ge complex [$(Et_3P)_2$PtN(Ph)OGe{$N(SiMe_3)_2$}$_2$], which has a long N−O bond (1.498(6) Å), may also be viewed as a μ-η^1:η^1-PhNO-*N,O* complex. See: Litz, K. E.; Kampf, J. W.; Holl, M. M. B. *J. Am. Chem. Soc.* **1998**, *120*, 7484−7492.

(24) (a) Gervasio, G.; Rossetti, R.; Stanghellini, P. L. *J. Chem. Soc., Chem. Commun.* **1977**, 387−388. (b) Scott, M. J.; Lippard, S. J. *Organometallics* **1998**, *17*, 466−474.

(25) Cameron, M.; Gowenlock, B. G.; Vasapollo, G. *J. Organomet. Chem.* **1991**, *325*, 325−333.

(26) (a) Swanwick, M. G.; Waters, W. A. *J. Chem. Soc. B* **1971**, 1059−1064. (b) Dinjus, E.; Walther, D.; Kirmse, R.; Stach, J. *J. Organomet. Chem.* **1980**, *198*, 215−224. (c) Lucas, D.; Mugnier, Y.; Antiñolo, A.; Otero, A.; Garcia-Yuste, S.; Fajardo, M. *J. Organomet. Chem.* **1995**, *490*, 7−10.

Ru, Rh, Ir) display reversible oxidation waves at significantly different potentials in the same solvent ($E_{1/2}$: M = Ru, 0.54 V; M = Rh, 1.04 V; M = Ir, 0.79 V vs SCE). This observation suggests that the electrochemical oxidation of the complexes **8**, **9a**, and **10a** occurs primarily at the nitrosobenzene ligand rather than the metal centers, and such assignment can be accounted for by the radical character of the nitrosobenzene ligand (Chart 1).

Unfortunately, reactivity of the coordinated nitrosobenzene in complexes **8**−**10** remains undeveloped. Their reactions with CO were investigated under CO pressure (30 atm, 120 °C), but formation of carbonylated organic products such as PhNCO was not confirmed by the GLC analysis of the reaction mixtures.

Reactions of the Chloro Complexes 1−3 with Nitrosobenzene. Reactions of cationic chloro complexes **1**−**3** with nitrosobenzene were also investigated. Although the diruthenium complex **1** failed to give characterizable products, the diiridium complex **3** reacted with nitrosobenzene at room temperature in THF to afford the nitrosobenzene complex **10a** in 35% yield. The dirhodium complex **2** did not react at room temperature, but unexpectedly, it was converted into the cationic trirhodium cluster $[(Cp^*Rh)_3(\mu\text{-}Cl)_2(\mu_3\text{-}S)(\mu\text{-}SPr^i)][OTf]$ (**11a**) by refluxing in THF with an excess amount of nitrosobenzene in good yield (eq 6). This cluster formation includes C−S bond cleavage of

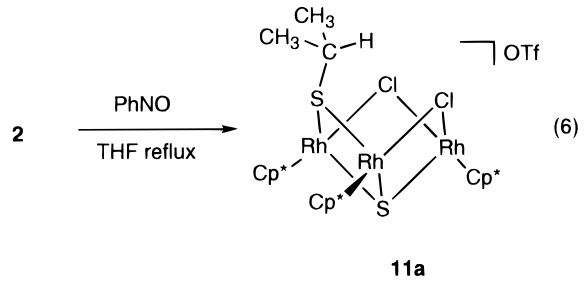

11a

one SPr^i ligand per a cluster molecule to provide the μ_3-S ligand.[27] However, attempts to clarify the fate of the Pr^i group by the GLC analysis of the gaseous and liquid products were unsuccessful. Azoxybenzene was the only organic product characterized in the liquid phase, and no more than a trace amount of propane was detected in the gas phase.

The molecular structure of the cluster was fully characterized by X-ray diffraction study of the $[BPh_4]^-$ salt $[(Cp^*Rh)_3(\mu\text{-}Cl)_2(\mu_3\text{-}S)(\mu\text{-}SPr^i)][BPh_4]\cdot 0.5(CH_3COCH_3)$ (**11b**·$0.5(CH_3COCH_3)$). The unit cell in the crystal of **11b**·$0.5(CH_3COCH_3)$ contained two independent cluster molecules, whose structures are essentially equivalent. An ORTEP drawing for one of the independent cations is given in Figure 4, and selected bond distances and angles are collected in Table 6. Cluster **11b** has a cuboidal trirhodium core, where the Rh_3 unit is capped by a μ_3-S ligand, and the Rh−Rh edges are bridged by two μ-Cl and one μ-SPr^i ligands. The long Rh−Rh separations (3.575(1)−3.590(1) Å) exclude any metal−metal bonding interactions, as expected from the total electron count of 54e$^-$. Although the sulfido and chloro ligands can hardly be distinguished on the basis of their difference in electron densities, the Rh−Cl (2.441(2)−2.480(2) Å) and Rh−μ_3-S (2.365(2)−2.377(2) Å) bond distances agreed very closely with the corresponding values reported for the related trirhodium complexes without Rh−Rh bonds $[Rh_3(\mu\text{-}Cl)_2(\mu_3\text{-}S)_2(\mu\text{-}S)(PEt_3)_6][PF_6]$ (Rh−Cl (av), 2.42 Å; Rh−μ_3-S (av), 2.379 Å)[28] and $[NMe_4][Rh_3(\mu_3\text{-}S)_2(CO)_6]$ (Rh−μ_3-S (av), 2.351 Å),[29] which supports the above assignment. While the Rh_4S_4 cubane cluster $[Cp^*_4Rh_4S_4]$[2c,27d] and some triangular rhodium clusters with two μ_3-S caps[28−30] have been described in the literature, the incomplete cubane-

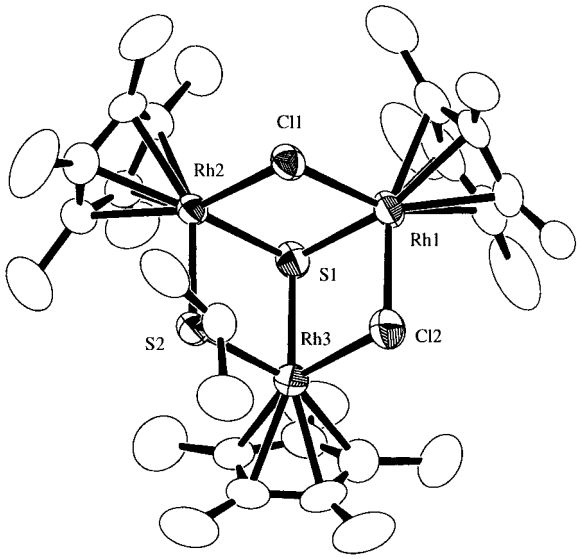

Figure 4. Structure of the cationic part in **11b**·$0.5(CH_3COCH_3)$. Hydrogen atoms are omitted for clarity.

Table 6. Selected Interatomic Distances and Angles in **11b**·$0.5(CH_3COCH_3)$

		Distances (Å)	
Rh(1)···Rh(2)	3.577(1)	Rh(1)···Rh(3)	3.575(1)
Rh(2)···Rh(3)	3.586(1)	Rh(1)−Cl(1)	2.445(2)
Rh(1)−Cl(2)	2.453(3)	Rh(1)−S(1)	2.365(2)
Rh(2)−Cl(1)	2.441(2)	Rh(2)−S(1)	2.371(2)
Rh(2)−S(2)	2.386(2)	Rh(3)−Cl(2)	2.468(2)
Rh(3)−S(1)	2.369(3)	Rh(3)−S(2)	2.382(2)
Rh(4)···Rh(5)	3.590(1)	Rh(4)···Rh(6)	3.584(1)
Rh(5)···Rh(6)	3.581(1)	Rh(4)−Cl(3)	2.461(2)
Rh(4)−Cl(4)	2.480(2)	Rh(4)−S(3)	2.377(2)
Rh(5)−Cl(3)	2.464(2)	Rh(5)−S(3)	2.368(2)
Rh(5)−S(4)	2.377(2)	Rh(6)−Cl(4)	2.458(2)
Rh(6)−S(3)	2.376(3)	Rh(6)−S(4)	2.384(2)
		Angles (deg)	
Cl(1)−Rh(1)−Cl(2)	92.11(8)	Cl(1)−Rh(1)−S(1)	83.80(7)
Cl(2)−Rh(1)−S(1)	84.51(8)	Cl(1)−Rh(2)−S(1)	83.75(8)
Cl(1)−Rh(2)−S(2)	93.00(8)	S(1)−Rh(2)−S(2)	82.00(8)
Cl(2)−Rh(3)−S(1)	84.08(8)	Cl(2)−Rh(3)−S(2)	94.00(8)
S(1)−Rh(3)−S(2)	82.13(8)	Rh(1)−Cl(1)−Rh(2)	94.10(8)
Rh(1)−Cl(2)−Rh(3)	93.17(8)	Rh(1)−S(1)−Rh(2)	98.09(8)
Rh(1)−S(1)−Rh(3)	98.09(9)	Rh(2)−S(1)−Rh(3)	98.30(9)
Rh(2)−S(2)−Rh(3)	97.52(9)	Cl(3)−Rh(4)−Cl(4)	93.10(8)
Cl(3)−Rh(4)−S(3)	83.95(8)	Cl(4)−Rh(4)−S(3)	84.15(7)
Cl(3)−Rh(5)−S(3)	84.04(8)	Cl(3)−Rh(5)−S(4)	94.11(8)
S(3)−Rh(5)−S(4)	82.33(7)	Cl(4)−Rh(6)−S(3)	84.64(7)
Cl(4)−Rh(6)−S(4)	92.86(8)	S(3)−Rh(6)−S(4)	82.01(8)
Rh(4)−Cl(3)−Rh(5)	93.61(8)	Rh(4)−Cl(4)−Rh(6)	93.09(7)
Rh(4)−S(3)−Rh(5)	98.34(9)	Rh(4)−S(3)−Rh(6)	97.90(8)
Rh(5)−S(3)−Rh(6)	98.00(8)	Rh(5)−S(4)−Rh(6)	97.57(8)

(27) The C−S bond rupture of thiolato ligands on transition metal complexes has been used for the sulfido cluster synthesis. For recent examples, see: (a) Matsubara, K.; Okamura, R.; Tanaka, M.; Suzuki, H. *J. Am. Chem. Soc.* **1998**, *120*, 1108−1109. (b) Curtis, M. D.; Druker, S. H. *J. Am. Chem. Soc.* **1997**, *119*, 1027−1036. (c) Firth, A. V.; Stephan, D. W. *Inorg. Chem.* **1997**, *36*, 1260−1262. (d) Feng, Q.; Krautscheid, H.; Rauchfuss, T. B.; Skaugset, A. E.; Venturelli, A. *Organometallics* **1995**, *14*, 297−304. (e) Coucouvanis, D.; A. Hadjikyriacou, A.; Lester, R.; Kanatzidis, M. G. *Inorg. Chem.* **1994**, *33*, 3645−3655.

(28) Cecconi, F.; Ghilardi, C. A.; Midollini, S.; Orlandini, A.; Vacca, A.; Ramirez, J. A. *Inorg. Chim. Acta* **1989**, *155*, 5−6.

(29) Galli, D.; Garlaschelli, L.; Ciani, G.; Fumagalli, A.; Martinengo, S.; Sironi, A. *J. Chem. Soc., Dalton Trans.* **1984**, 55−61.

type $Rh_3S_nX_{4-n}$ cluster core is unprecedented. The Pr^i group occupies an axial-like position of the six-membered ring formed by the three rhodium, two chlorine, and one thiolato sulfur atoms. This orientation of the Pr^i group avoids steric congestion between the Pr^i and Cp* groups, but in compensation for this, the methine proton of the Pr^i group is located unusually close to the chloro ligands[31] where the H···Cl distances (estimated to be 2.70−2.85 Å) are shorter than the sum of their van der Waals radii (2.95 Å).[32] In harmony with this crystal structure, **11a** is diamagnetic, and its ^{1}H NMR spectrum showed two Cp* signals at δ 1.54 and 1.55 in the intensity ratio of 1:2.

Finally, cyclic voltammogram of cluster **11a** was measured. In CH_2Cl_2/0.1 M $[Bu_4N][BF_4]$, **11a** showed two quasi-reversible oxidation waves overlapping with each other at $E_{pa} = 1.10$ and 1.27 V and $E_{pc} = 0.89$ and 1.04 V as well as two irreversible reduction waves at $E_p = -1.22$ and -1.50 V (vs SCE). The quasi-reversible waves can be assigned to the $Rh(III)_3$/$Rh(III)_2Rh(IV)$ and $Rh(III)_2Rh(IV)$/$Rh(III)Rh(IV)_2$ couples. Further reactivities of cluster **11** are now under investigation.

Acknowledgment. This work was supported by a Grant-in-aid for Specially Promoted Research (09102004) from the Ministry of Education, Science, Sports, and Culture, Japan.

Supporting Information Available: X-ray crystallographic files, in CIF format, for the structure determinations of **5**, **6b**·0.5(CH_2Cl_2), **7b**, **8**, **9b**, **10b**, and **11b**·0.5(CH_3COCH_3). This material is available free of charge via the Internet at http://pubs.acs.org.

IC981274E

(30) (a) Bright, T. A.; Jones, R. A.; Koschmieder, S. U.; Nunn, C. M. *Inorg. Chem.* **1988**, *27*, 3819−3825. (b) Arif, A. M.; Hefner, J. G.; Jones, R. A.; Koschmieder, S. U. *Polyhedron* **1988**, *7*, 561−572. (c) Nishioka, T.; Isobe, K. *Chem. Lett.* **1994**, 1661−1664.

(31) Similar intramolecular close contacts between a CH group and S atoms have been reported for a trinuclear ruthenium complex. See: Shaver, A.; Plouffe, P.-Y.; Liles, D. C.; Singleton, E. *Inorg. Chem.* **1992**, *31*, 997−1001.

(32) Bondi, A. *J. Phys. Chem.* **1964**, *68*, 441−451.